**Supplemental information**

This file includes:

Figures S1 to S7
Tables S1 to S5

# E3 ubiquitin-protein ligase TRIM21-mediated lysine capture by UBE2E1 reveals substrate-targeting mode of a ubiquitin-conjugating E2

**Madhanagopal Anandapadamanaban[1,2], Nikolaos C. Kyriakidis[3,4#], Veronika Csizmók[1#], Amélie Wallenhammar[1], Alexander C. Espinosa[3], Alexandra Ahlner[1], Adam R. Round[5,6], Jill Trewhella[1,7], Martin Moche[8], Marie Wahren-Herlenius[3] & Maria Sunnerhagen[1]***

From the [1]Department of Physics, Chemistry and Biology, Division of Chemistry, Linköping University, SE-58183 Linköping, Sweden
[3]Unit of Experimental Rheumatology, Department of Medicine, Karolinska Institutet, Karolinska University Hospital, 17176 Stockholm, Sweden
[5]European Molecular Biology Laboratory, Grenoble Outstation, 6 rue Jules Horowitz, 38042 Grenoble, France
[7]School of Life and Environmental Sciences (SoLES), The University of Sydney, NSW 2006, Australia
[8] Department of Medical Biochemistry and Biophysics, Protein Science Facility, Karolinska Institutet, SE-17177 Stockholm, Sweden.

# These authors contributed equally to this work.
[2]Present address: Medical Research Council, Laboratory of Molecular Biology, Cambridge Biomedical Campus, Francis Crick Ave., Cambridge CB2 0QH, UK
[4]Present address: Escuela de Medicina, Facultad de Ciencias de la Salud, Grupo de Investigación en Biotecnología Aplicada a Biomedicina (BIOMED), Universidad de Las Américas (UDLA), Quito, Ecuador
[6] Present address: European XFEL GmbH, Holzkoppel 4, 22869 Schenefeld, Germany

*To whom correspondence should be addressed: Maria Sunnerhagen, maria.sunnerhagen@liu.se

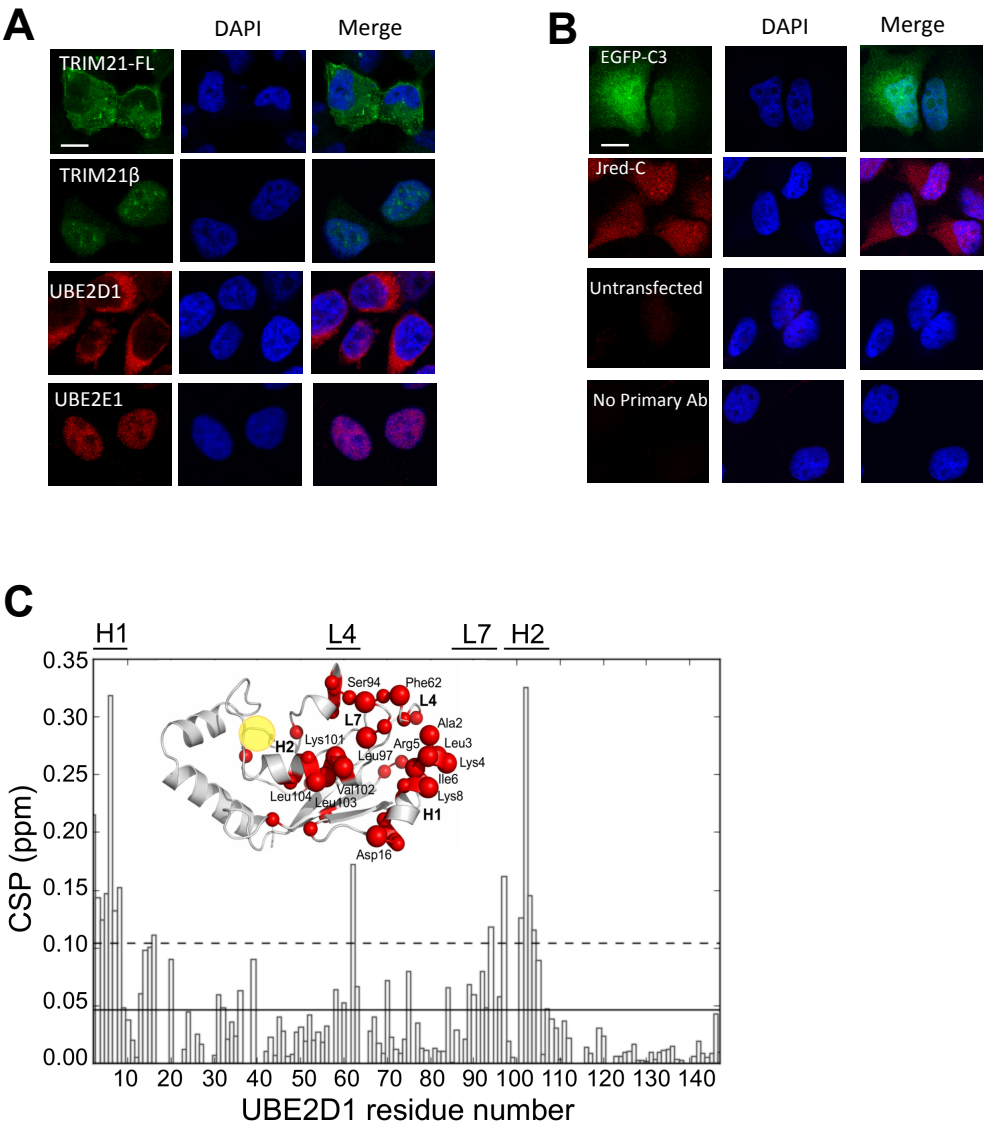


**Figure S1. Intracellular localization of TRIM21 isoforms, UBE2D1 and UBE2E1 in HeLa cells.**

(**A**) Intracellular localization of TRIM21 isoforms with UBE2D1 or UBE2E1 in HeLa cells. DAPI blue staining shows EGFP-TRIM21 mainly located in the cytoplasm and at low levels in the nucleus, whereas EGFP-TRIM21β is located mainly in the nucleus. JRed-UBE2D1 localized to the cytoplasm as does EGFP-TRIM21, whereas JRed-UBE2E1 is almost exclusively localized in the nucleus, suggesting a possible co-localization with the EGFP-TRIM21β isoform. Scale bar, 10 μm. (**B**) Experimental controls: Transfection of HeLa cells with 500 ng of EGFP-C3 or Jred-C empty vectors resulted in an evenly distributed expression pattern of the fluorescent tags. Untransfected cells emitted no signal both in the green and the red spectra. Similar results were obtained with immunofluorescent staining of HeLa cells with PBS replacing the rabbit anti-human UBE2E1 antibody. (**C**) Combined $^{1}H$ and $^{15}N$ CSPs of UBE2D1 upon $TRIM21_{R}$ binding; solid/dashed lines and inset as in Figure. 1F. The E2 active site is highlighted (yellow sphere).

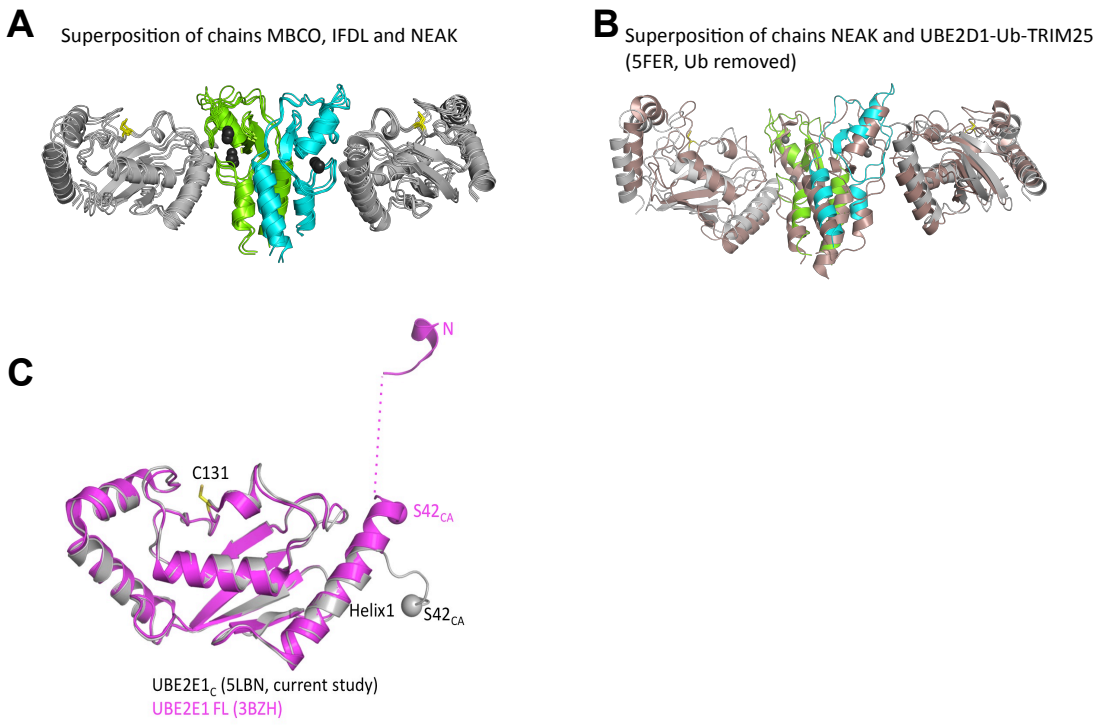


**Figure S2. Structural assembly of the TRIM21$_R$-UBE2E1$_C$ complex.**
(**A**) Superpositions of TRIM21$_R$-UBE2E1$_C$ complete 2:2 complexes. (**B**) Superpositions of E2s on TRIM21$_R$-UBE2E1$_C$ and UBE2D1-Ub-TRIM25 complex (PDB ID 5FER). (**C**) UBE2E1$_C$ (current study, grey) superimposed onto the core domain (residue 46-193) of full-length UBE2E1 (PDB ID 3BZH, magenta), resulting RMSD value of 0.44. The c-alpha residue of S42 is shown in both E2 structure in sphere highlighting the N-terminal variation.

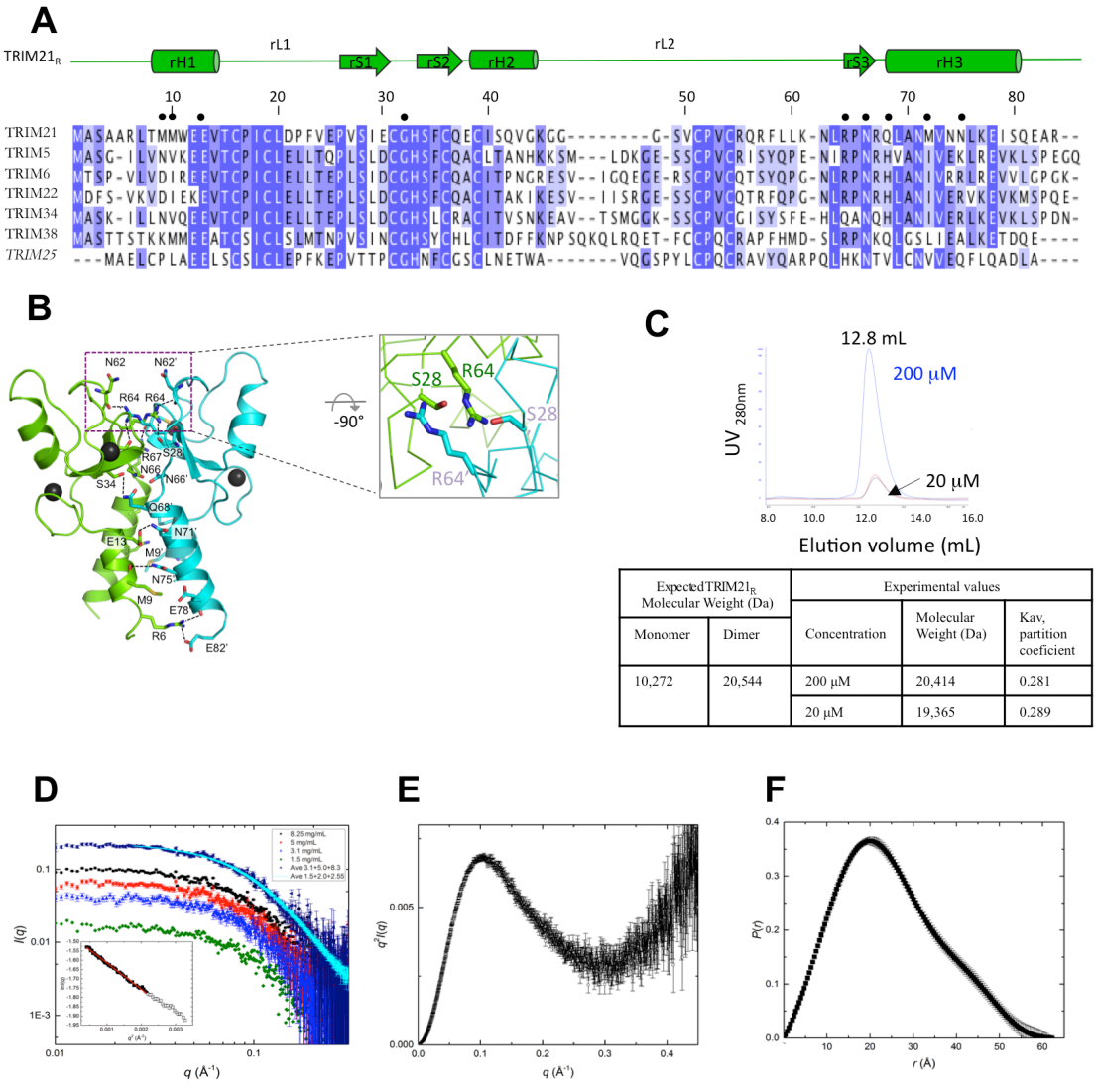


| Expected TRIM21R Molecular Weight (Da) | | Experimental values | | |
|---|---|---|---|---|
| Monomer | Dimer | Concentration | Molecular Weight (Da) | Kav, partition coeficient |
| 10,272 | 20,544 | 200 µM | 20,414 | 0.281 |
| | | 20 µM | 19,365 | 0.289 |

**Figure S3. Solution structure and interface of TRIM21R dimer.** (**A**) Sequence and secondary structure in TRIM21R, together with sequence alignment to TRIM5, TRIM6, TRIM22, and TRIM34 (Chromosome 11), TRIM38 (Chromosome 6) and TRIM25 (Chromosome 17). The classic "RING" comprises residues 16-55 in TRIM21. are shown together with the alignment of TRIM proteins. (**B**) The TRIM21R homodimer is shown, highlighting residues with reduced accessible surface according to VADAR analysis (Willard, 2003) (> 10%; annotated) and interfacial hydrogen bonds (hatched lines). A reciprocal interaction network across the TRIM21 interface involves Ser28/28'-Arg64'/64 (inset). (**C**) Analytical gel filtration chromatogram for TRIM21R at two different concentrations (200 µM and 20 µM) show the corresponding elution as a dimer (Table inset). Using the experimental standard plot (see Methods) the elution profiles of TRIM21R chromatogram corresponds to a molecular weight of 20.4 kDa, which corresponds well to that of a dimer (gel phase distribution coefficient, $K_{av}$ 0.28). (**D**) $I(q)$ vs $q$ as log-log plots show the flattening at low-$q$ , indicating the data were measured to sufficiently low-$q$ to characterise the longest dimensions in the sample which was free of non-specific aggregation. Symbols represent SAXSess data measured in buffer containing 10% glycerol; concentrations such as 1.5 mg/ml (green), 3.1 mg/ml (blue), 5 mg/ml (red) and 8.25 mg/ml (black), measured on the Anton Paar SAXSess benchtop instrument. The cyan line represents the averaged ESRF data, which is in excellent agreement with the averaged SAXSess data (symbol), showing excellent agreement between the two independent measurements. Inset showing Guinier plot is for the ESRF 1.5, 2.0, 2.55 mg/mL averaged data, starting at the minimum q specification for BL29 and extending to qRg

= 1.3. The filled symbols with the red fitted line is the Guinier region and the open symbols show points beyond the Guinier region. The Pearson's R2 coefficient is 0.997 indicating a good linear fit. (**E**) Kratky plot for $TRIM21_R$ subunit in solution, ESRF Averaged 1.5, 2.0, 2.55 mg/mL data show the initial bell shape characteristic of a folded protein with a strong upturn at high-$q$, indicating a portion of the structure is flexible. (**F**) $P(r)$ versus $r$ for $TRIM21_{1\text{-}91}$ in solution, SAXSess data averaged for 3.1, 5, 8.3 mg/mL was used given the significantly lower $q_{min}$ for these data improved the reliability of the bead modelling**.**

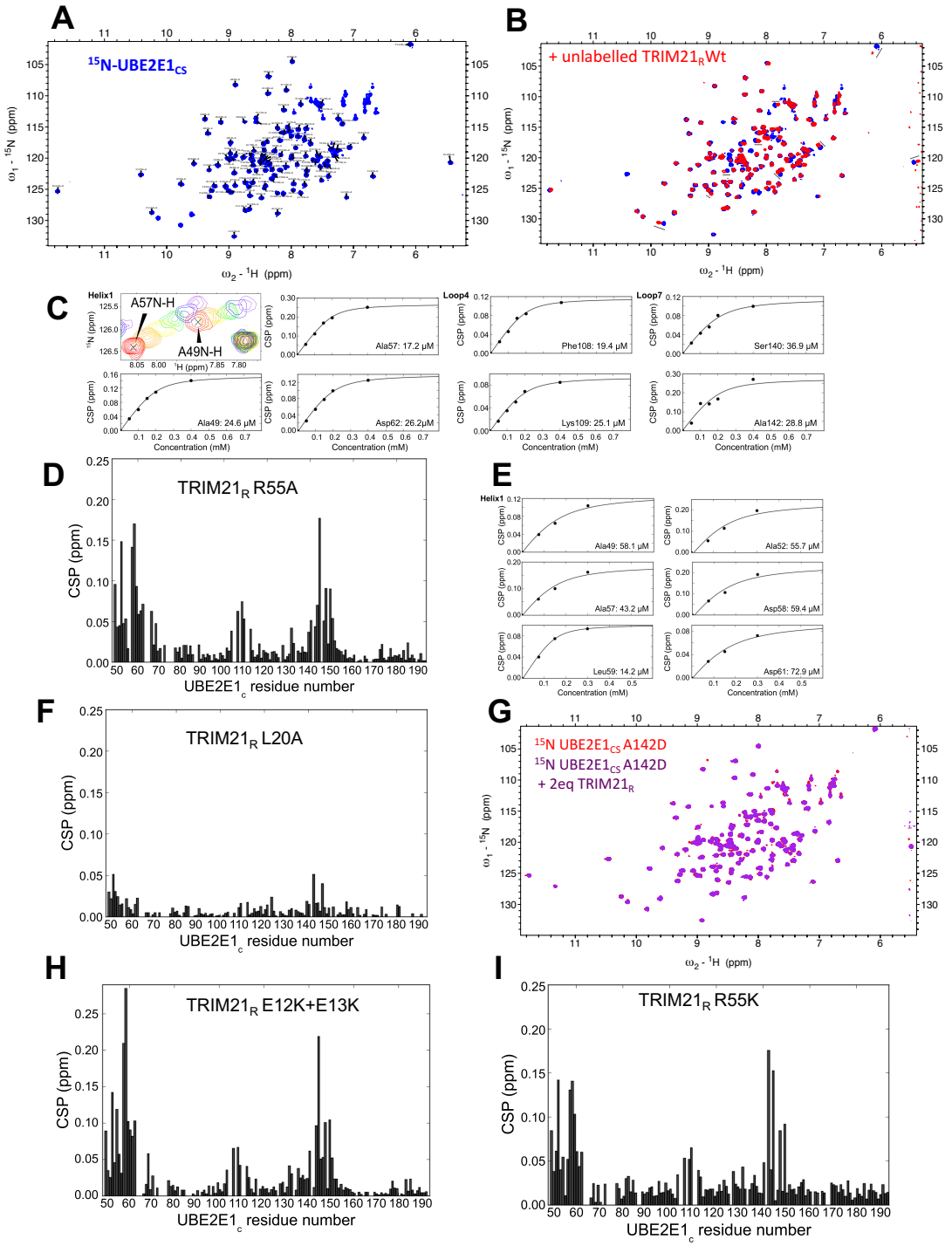


**Figure S4: HSQCs of $^{15}$N UBE2E1$_{CS}$ binding to unlabelled TRIM21$_R$ wt and mutants.** (**A**) $^1$H, $^{15}$N-TROSY-HSQC of $^{15}$N-UBE2E1$_{CS}$ (blue spectrum), with assigned residues labelled. For all NMR analysis, a UBE2E1$_{CS}$ construct containing a mutation of the active cysteine (C131S) was used. (**B**) $^1$H, $^{15}$N-TROSY-HSQC of 15N-UBE2E1$_{CS}$ + 2 equivalents of TRIM21$_R$ (red spectrum), overlaid on the spectrum of 15N-UBE2E1$_{CS}$ (blue). Residues affected by the interaction visibly show significant peak shifts; the less clear shifts highlighted with a straight indicator line. (**C**) Chemical shift perturbations (CSPs) fitted (black line) to calculate the apparent Kd (inserted). (**D**) CSPs of $^{15}$N UBE2E1$_{CS}$ in presence of 2.0 eq TRIM21$_R$ mutants R55A. (**E**) CSPs in titrations of 15N-UBE2E1$_{CS}$ with the unlabeled TRIM21$_R$ R55A mutant are shown for some residues. (**F**) CSPs of $^{15}$N UBE2E1$_C$ in presence of 2.0 eq TRIM21$_R$ mutants L20A. (**G**) Overlay of $^{15}$N UBE2E1$_{CS}$ A142D in the absence (red)

or presence (magenta) of 2 molar equivalents of an unlabelled $TRIM21_R$ indicates no binding. See Methods for details. NMR analysis of $^{15}N$ UBE2D1 WT and $^{15}N$ $UBE2E1_{CS}$ binding to unlabelled $TRIM21_R$ mutants. CSPs of $^{15}N$ $UBE2E1_{CS}$ in the presence of 2.0 eq unlabelled $TRIM21_R$ wild-type (black) as a function of sequence (black), together with CSPs of $^{15}N$ $UBE2E1_{CS}$ in presence of 2.0 eq $TRIM21_R$ mutants (red). The following $TRIM21_R$ mutants were analysed (**H**) a double mutant E12+13/K and (**I**) a R55K mutant.

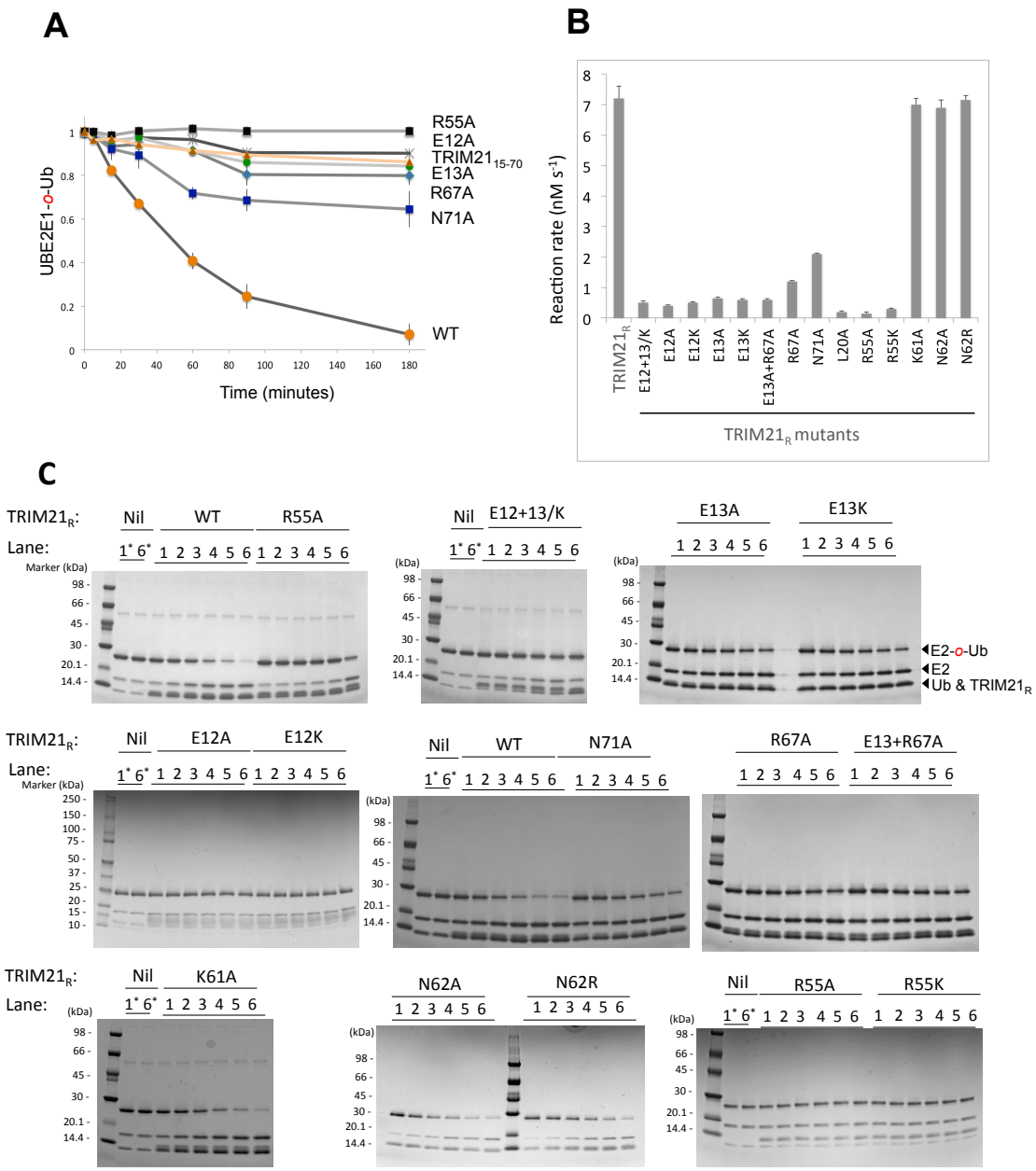


**Figure S5**. **E2-*o*-Ub oxyester hydrolysis assay**
(**A**) TRIM21-mediated hydrolysis of UBE2E1$_C$ (C131S)–Ub oxyester using wt and mutated TRIM21$_R$. No hydrolysis occurred in the absence of TRIM21$_R$, or in the presence of TRIM21$_R$ with a mutated R55A "linchpin" residue, ensuring that the hydrolysis of the oxyester bond is completely dependent on the presence of an E3 catalytic element. (**B**) Reaction rates were calculated from the slopes of the linear phase showing the hydrolysis of E2~Ub oxyester band by fitting the quantified intensities as a function of time. The quantified intensities are averaged as the mean ± s.d. of triplicate experiments. The sample without an E3 (TRIM21$_R$) was used as a standard and this correspond to the concentration of E2~Ub oxyester at the start of the reaction measured using UV absorbance at 280nm. (**C**) Coomasie-stained SDS-PAGE gels of the above oxyester conjugate and analysis of the respective TRIM21$_R$ mutants at increasing time points. The variables are annotated in the SDS-PAGE gels.

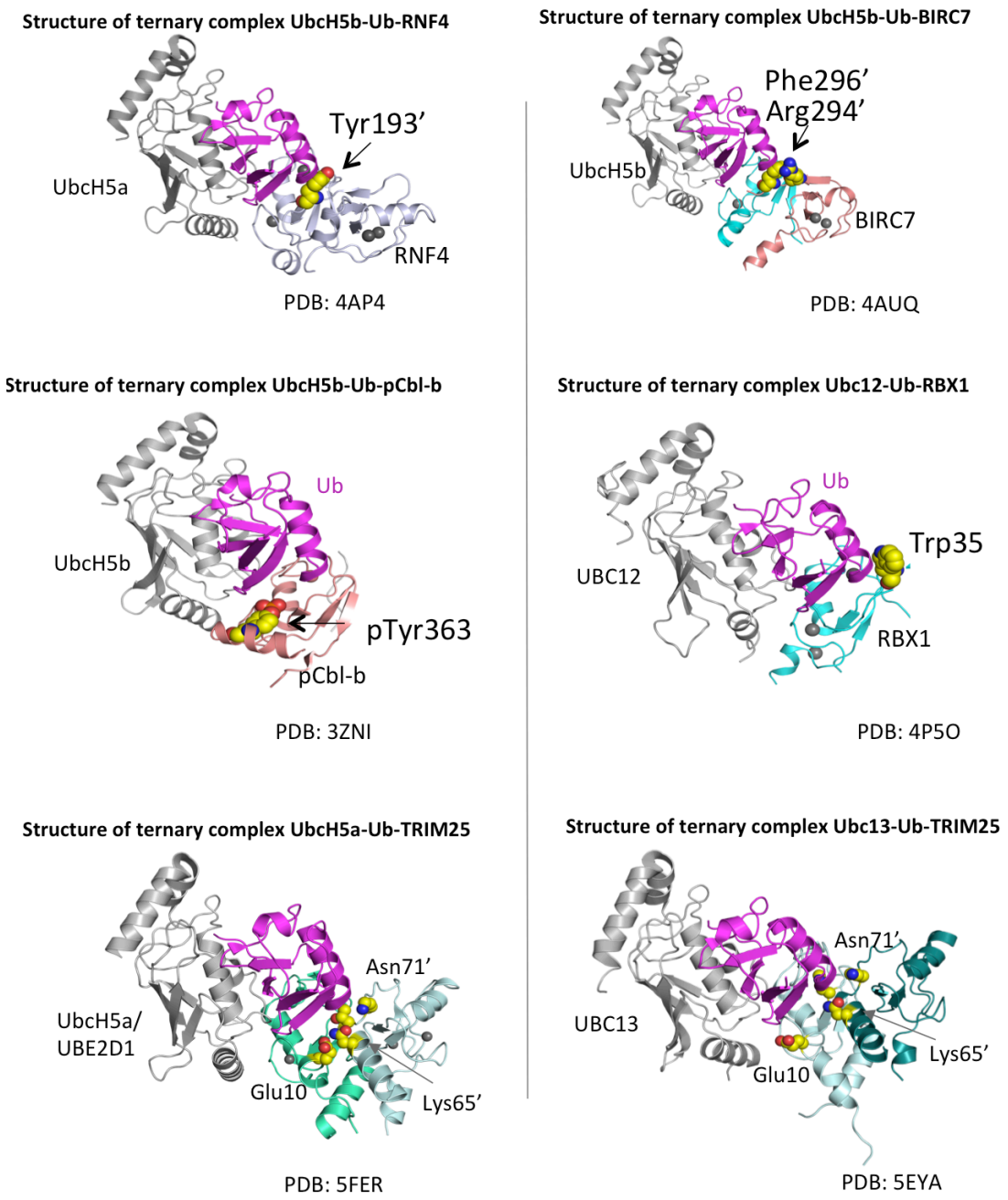


**Figure S6. A graphical review of ubiquitin recognition by RING E3 ligases.**
The interactions between RING-type E3 ligases and the donor ubiquitin are shown in a series of RING-type E2-Ub-E3 ternary complexes displayed in similar orientations (Dou et al., 2013; 2012b; Koliopoulos et al., 2016; Plechanovová et al., 2012; Pruneda et al., 2012; Sanchez et al., 2016; Taherbhoy et al., 2015; PDB IDs as annotated). In each structure, contacting residues from E3 to donor Ub are shown in spheres and annotated.

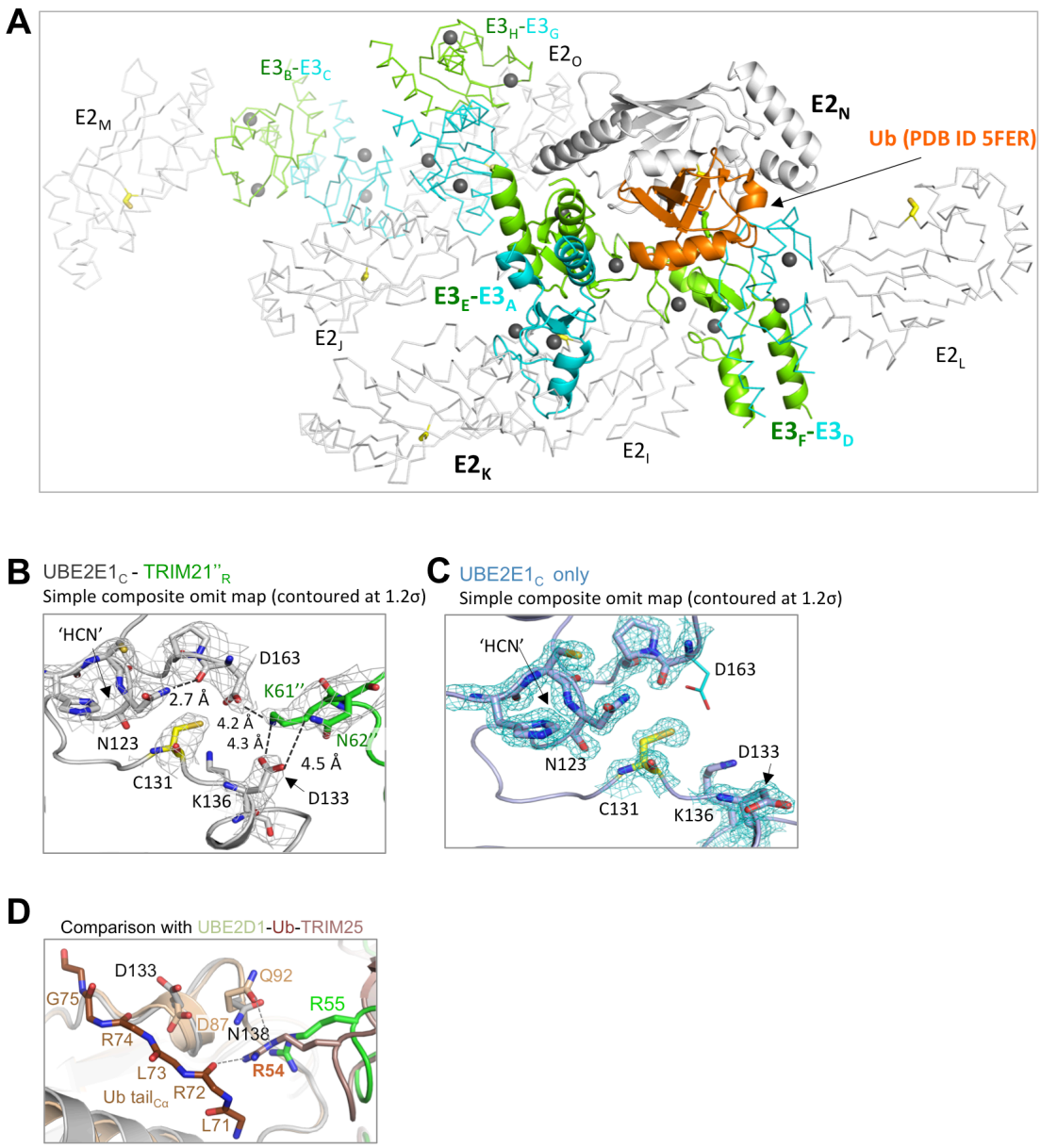


**Figure S7. Supporting data for Ub model and substrate complex**

(**A**) Same as Supplementary Figure.1A, with the donor Ub (orange) modelled onto the E2 chain-N. The Ub model is obtained by superposition of E2's from the TRIM25-UbcH5-Ub to our structure of chain NEA, as in Figure. 3. The closed-state Ub can be modeled into the structure without clashes, together with the entire NEAF chain assembly, and in the same asymmetric unit. Together, this jointly supports that the crystal structure reflects the properties of a functionally relevant multidomain assembly rather than a collapsed aggregate of domains.

Composite omit 2fo-fc map are shown for UBE2E1-TRIM21 (**B**) and UBE2E1 only (**C**) structures, contoured at 1.2 sigma. This omit map figure is produced as similar to our Main Fig. 3B and 3F. A composite omit 2fo-fc map was made using phenix 1.13-2998 software (Afonine, P.V. et al. FEM: feature-enhanced map. Acta Crystallog r D Biol Crystallogr **71**, 646-66 (2015).

(**D**) UBE2E1$_C$-TRIM21$_R$ complex (chains NEA) superimposed on the TRIM25(copper)-UBE2D1(gold)~Ub(brown) (PDB ID **5FER**) ternary complex by their respective E2 coordinates (Cα RMSD of 0.54Å). Orientation as in (I). Black dashed lines indicate hydrogen bonds connecting TRIM25-R54 ("linchpin") to E2 and to the Ub c-terminal tail.

**Table S1: List of $C_\alpha$ RMSDs to its relative chains and the complex that they form as indicated.**

Superposition of the $TRIM21_R$-$UBE2E1_C$ 2:2 complex (chains NEAK) onto the TRIM25-UBE2D1 crystal structure (PDB id: 5FER, Ub chain is removed). Supplementary Table 1 lists the corresponding RMSDs between protomers and assemblies described in Supplementary Fig.1a.

| **Main chain** | **Aligning chain** | **Cα RMSDs** |
|---|---|---|
| **E2 chains:** (146 residues are aligned) | | |
| E2 (chain N) | E2 chain I,J,K,L,M,O | 0.26+/-0.03 |
| | $UBE2E1_C$ alone (this study, 5LBN) | 0.38 |
| | $UBE2E1_{full\text{-}length}$ (3BZH, residues 42-193) | 0.46 |
| $UBE2E1_{core}$ alone (this study, 5LBN) | $UBE2E1_{full\text{-}length}$ (3BZH, residues 42-193) | 0.47 |
| **RING dimers:** (150 residues are aligned) | | |
| RING chain EA | RING chain FD,BC, HG | 0.43+/-0.17 |
| **Overall Cα RMSDs for 2:2 complexes, E2-$TRIM21_R$-E2:** (401 residues are aligned) | | |
| chain NEAK | chain MBCO | 0.92 |
| | chain IFDL | 1.2 |
| | 5FER (UBE2D1-Ub-TRIM25), Ub removed | 3.2 |
| chain MBCO | chain IFDL | 1.8 |
| **E2 C✔ RMSDs for 1:2 complexes (E2-$TRIM21_R$)** (306 residues are aligned) | | |
| chain NEA | chain LFD, IFD, KEA, JHG, OBC, MBC | 0.26+/-0.03 |

**Table S2: Interacting residues and hydrogen bond distance in the $TRIM21_R$-$UBE2E1_C$ interface (chain NEA as in Main Fig. 1A).** PDBePISA (Protein Interfaces, Surfaces and Assemblies) was used to identify the hydrogen bonds and calculate the distance.

| **$UBE2E1_C$-$TRIM21_R$ interface (chain NE)** | | |
|---|---|---|
| Hydrogen Bonds | | |
| N:ARG 51[ NH1] | 3.54 | E:PRO 17[ O ] |
| N:ARG 51[ NH1] | 2.49 | E:ILE 18[ O ] |
| N:LYS 54[ NZ ] | 3.37 | E:ILE 18[ O ] |
| N:SER 140[ OG ] | 2.72 | E:PRO 52[ O ] |
| N:ASN 138[ OD1] | 3.38 | E:ARG 55[ NE ] |
| N:ASN 138[ O ] | 2.89 | E:ARG 55[ NH2] |
| Salt Bridges | | |
| N:LYS 54[ NZ ] | 3.37 | E:ASP 21[ OD1] |
| N:LYS 50[ NZ ] | 3.61 | E:ASP 21[ OD2] |
| **$TRIM21_R$ homodimer interface (chain EA)** | | |
| Hydrogen Bonds | | |
| A:ASN 75[ ND2] | 3.45 | E:MET 9[ O ] |
| A:ASN 71[ ND2] | 2.96 | E:GLU 13[ OE1] |
| A:ARG 64[ NH1] | 2.98 | E:SER 28[ O ] |
| A:ARG 64[ NH1] | 3.27 | E:SER 28[ OG ] |
| A:ARG 64[ NH2] | 2.68 | E:ASN 62[ O ] |
| A:ASN 66[ ND2] | 2.81 | E:ASN 66[ OD1] |
| A:GLU 78[ O ] | 3.28 | E:ARG 6[ NH1] |
| A:GLU 82[ OE2 | 2.53 | E:ARG 6[ NH1] |
| A:GLU 78[ O ] | 3.41 | E:ARG 6[ NH2] |
| A:GLN 68[ OE1] | 3.59 | E:SER 34[ OG ] |
| A:SER 28[ OG ] | 2.67 | E:ARG 64[ NH1] |
| A:ASN 62[ O ] | 2.80 | E:ARG 64[ NH2] |
| A:ASN 66[ OD1] | 2.93 | E:ASN 66[ ND2] |
| A:CYS 31[ O ] | 3.20 | E:ARG 67[ NH2] |
| A:GLU 13[ OE1] | 2.87 | E:ASN 71[ ND2] |
| A:MET 9[ O ] | 3.51 | E:ASN 75[ ND2] |
| Salt Bridges | | |
| A:ARG 64[ NH2] | 3.96 | E:GLU 30[ OE1] |
| A:GLU 82[ OE2] | 2.53 | E:ARG 6[ NH1] |

**Table S3. SAXS data acquisition, sample details and software employed.**

| **(a) Data collection parameters** | | |
|---|---|---|
| Instrumentation | ESRF | Anton Paar SAXSess |
| Beam geometry | 250 μm × 150 μm | 10 mm line, AH=0.24, LH=0.12* |
| $q$-range measured ($Å^{-1}$) | 0.02-0.5 $Å^{-1}$ | 0.009-0.63 |
| Exposure time (seconds) | 5 s x 10 | 4 x 15 min |
| Temperature ($^{o}C$) | 20 | 20 |
| *Parameters input to GNOM for trapezoidal approximation for slit beam geometry | | |

| **(b) Sample details** | | |
|---|---|---|
| | $TRIM21_R$ | |
| Molar ratio in $UBE2E1_{core}$:$TRIM21_{1-91}$ complex | - | |
| Contrast from sequence and solvent constituents ($\Delta\rho$, $10^{10}$ $cm^{-2}$) | 3.078** | |
| Partial specific volume from sequence ($v$, $cm^3$ $g^{-1}$) | 0.721 | |
| Molecular weight from sequence | 10410 (monomer) | |
| ** $TRIM21_R$ samples measured using the SAXSess included 10% glycerol in buffer | | |

| **(c) Software employed for data reduction, analysis and interpretation** | |
|---|---|
| SAXS data reduction to $I(q)$ v $q$ | SAXSQuant (Anton Paar) for SAXSess and as described at ref [86] |
| Calculation of $M_r$, $\Delta\rho$ and $\vartheta$ values from sequence | MULCh[82] |
| SAXS data processing and analysis: Guinier and $P(r)$ | ATSAS 2.7.1 SAS Data Analysis[83] |
| *ab initio* bead modelling | DAMMIF[85] (via ATSAS on-line) |
| Crystal structure fits to data | CRYSOL[84] |
| 3D graphic model representations | PyMol Molecular Graphics System, Version 1.2r3pre (Schrödinger) |

**Table S4. SAXS-derived structural parameters for $TRIM21_R$**

| **ESRF BL29 Data** | | | **SAXSess Data** | |
|---|---|---|---|---|
| Guinier Analysis | | | | |
| Protein concentration (mg/mL) | $R_g$ (Å) for $qR_g$ < 1.3 | Molecular mass, $M_r$, from $I(0)$ values* (ratio to expected value for the monomer) | Protein concentration (mg/mL) | $R_g$ (Å) for $qR_g$ < 1.3 |
| 1.5 | 19.6 ± 0.1 | 17121 (1.64) | 1.5 | 19.4 ± 0.6 |
| 2.0 | 19.5 ± 0.1 | 18334 (1.76) | 3.1 | 19.1 ± 0.7 |
| 2.55 | 19.9 ± 0.1 | 18344 (1.76) | 5.0 | 18.4 ± 0.7 |
| Average of 1.5, 2.0, 2.55 | 19.7 ± 0.4 | - | 8.3 | 19.2 ± 0.6 |
| | | | Average of 3.1, 5.0, 8.3 | 18.8 ± 0.3 |
| P(r) analysis | | | | |
| Protein concentration (mg/mL) | $R_g$ (Å) | $d_{max}$ (Å) | $R_g$ (Å) | $d_{max}$ (Å) |
| 1.5 | 20.30 ± 0.02 | 80 | 18.9 ± .04 | 60 |
| 2.0 | 20.49 ± 0.01 | 80 | 19.0 ± 0.04 | 57 |
| 2.55 | 20.68 ± 0.01 | 80 | 19.2 ± 0.03 | 60 |
| Average of 1.5, 2.0, 2.55 | 20.54 ± 0.01 | 80 | 19.4 ± 0.04 | 60 |
| | | | 19.2 ± 0.03 | 62 |

* SAXSQuant desmeared data used for SAXSess analyses. Molecular weight values determined using $M_r = \frac{I(0) N_A}{c \rho_M^2}$ where $N_A$ = Avogadro's number, C = protein concentration (g/mL), $\Delta\rho_M = \Delta\rho\vartheta$ and $\Delta\rho$ = contrast in $cm^{-2}$ and $\vartheta$ = partial specific volume $cm^3/g$

**Table S5. List of the distances of acceptor residue to the active Cys for the known structures of E2-Ub/Ubl-E3-Substrate (PDB ids are annotated).**

| **Structures* (PDB ID)** | **E3** | **E2** | **Substrate** | **Acceptor residue** | **Distance from acceptor amide to E2 active Cys** |
|---|---|---|---|---|---|
| 6FGA, this study | TRIM21 | UBE2E1 | $TRIM21_R$ | K61" | 5.3 Å |
| 6FGA, with modeled K61" | TRIM21 | UBE2E1 | $TRIM21_R$ | K61" | 4.4 Å |
| 5JNE | SIZ1 | UBC9 | PCNA | K164 (C in structure) | 5.6 Å |
| 2GRN | - | UBC9 | RANGap1 | K524 | 3.4 Å |
| 4P5O | RBX1 | UBC12 | CUL1 | K720 (R in structure) | 5.25 Å |

*Structures of E2s in complex with donor and acceptor Ub(K63) are not included.